中国光学 Chinese Optics 核心期刊

湍流大气对光束相干合成效果的影响

宋纪坤 李远洋 车东博 郭劲 王挺峰 李志来

Influence of turbulent atmosphere on the effect of coherent beam combining

SONG Ji-kun, LI Yuan-yang, CHE Dong-bo, GUO Jin, WANG Ting-feng, LI Zhi-lai

引用本文:
宋纪坤, 李远洋, 车东博, 郭劲, 王挺峰, 李志来. 湍流大气对光束相干合成效果的影响[J]. 中国光学, 2020, 13(4): 884–898. doi: 10.37188/CO.2019–0197
SONG Ji-kun, LI Yuan-yang, CHE Dong-bo, GUO Jin, WANG Ting-feng, LI Zhi-lai. Influence of turbulent atmosphere on the effect of coherent beam combining[J]. *Chinese Optics*, 2020, 13(4): 884-898. doi: 10.37188/CO.2019-0197

在线阅读 View online: https://doi.org/10.37188/CO.2019–0197

文章编号 2095-1531(2020)04-0884-15

Influence of turbulent atmosphere on the effect of coherent beam combining

SONG Ji-kun[1,2], LI Yuan-yang[1], CHE Dong-bo[1,2], GUO Jin[1], WANG Ting-feng[1*], LI Zhi-lai[3]

(1. *State Key Laboratory of Laser Interaction with Matter*, *Changchun Institute of Optics*, *Fine Mechanics and Physics*, *Chinese Academy of Sciences*, *Changchun* 130033, *China*;;

2. *University of Chinese Academy of Sciences*, *Beijing* 100049, *China*;

3. *Space Optical Department Ⅱ*, *Changchun Institute of Optics*, *Fine Mechanics and Physics*, *Chinese Academy of Sciences*, *Changchun* 130033, *China*)

* *Corresponding author*, *E-mail*: *wangtingfeng@ciomp.ac.cn*

Abstract: Coherent beam combining is a promising technology for achieving a high-power laser beam with good beam quality. However, turbulent atmosphere is one of the key factors that restrict its application and development. This paper focuses on the influence of atmospheric Greenwood frequency on the correction effect of the coherent combination system based on Stochastic Parallel Gradient Descent (SPGD) algorithm. At first, the influence of different turbulence intensities on the correction effect of coherent combination systems is analyzed by numerical simulation under static atmospheric conditions. Then, a set of rotating phase screens that meet Kolmogorov's statistical law are generated by numerical calculation to simulate the turbulent atmosphere and study the correction effect of coherent combination system at different atmospheric Greenwood frequencies. Finally, an experimental platform is established to demonstrate the coherent combination effect of two laser beams. The simulated and experimental results show that when the system's control algorithm iteration frequency (350 Hz) is constant, the disturbance of turbulent atmosphere to the phase and light intensity of laser beams will increase with atmospheric Greenwood frequency, making the effect of coherent combination worse.

Key words: coherent beam combining; SPGD algorithm; turbulent atmosphere; phase screen

---

收稿日期:2019-10-08; **修订日期**:2019-11-09

基金项目:国家重点研发计划资助项目(No. 2016YFB0500100);国家自然科学基金资助项目(No. 61805234);激光与物质相互作用国家重点实验室基金项目(No. SKLLIM1704);中国科学院前沿科学重点研究项目(No. QYZDB-SSW-SLH014);民用航天预研项目(No. D040101)

Supported by National Key R&D Program of China (No. 2016YFB0500100); National Natural Science Foundation of China (No. 61805234); Fund of the State Key Laboratory of Laser Interaction with Matter (No. SKLLIM1704); Key Research Program of Frontier Sciences, CAS(No. QYZDB-SSW-SLH014); Civil Aerospace Pre-research Project (No. D040101)

湍流大气对光束相干合成效果的影响

宋纪坤[1,2], 李远洋[1], 车东博[1,2], 郭　劲[1], 王挺峰[1*], 李志来[3]
（1. 中国科学院 长春光学精密机械与物理研究所 激光与物质相互作用国家重点实验室，吉林 长春 130033；
2. 中国科学院大学，北京 100049；
3. 中国科学院 长春光学精密机械与物理研究所 空间光学研究二部，吉林 长春 130033）

摘要: 光纤激光相干合成是获得高功率高光束质量输出较为有效的途径，而湍流大气是制约其应用与发展的关键因素之一。本文重点研究了大气格林伍德频率对基于随机并行梯度下降算法（SPGD）相干合成系统校正效果的影响。首先，在静态大气条件下，分析了不同湍流强度对相干合成系统校正效果的影响；然后，利用数值计算生成一组旋转的符合Kolmogorov 统计规律的相位屏模拟湍流大气，对在不同大气格林伍德频率下相干合成系统的校正效果进行研究；最后，搭建两路光纤激光相干合成实验平台，进行实验验证。仿真和实验结果表明，在系统的控制算法迭代频率（350 Hz）一定时，随着大气格林伍德频率的增加，湍流大气对光束的相位和光强的扰动加剧，使得相干合成系统的合成效果变得越来越差。

关　键　词: 相干合成；SPGD 算法；湍流大气；相位屏
中图分类号: TN249　　**文献标志码:** A　　**doi:** 10.37188/CO.2019-0197

1　Introduction

Coherent beam combining of fiber laser array is the coherent superposition of sub-beams, which can greatly improve the output optical power and ensure good beam quality. It has a broad application prospect in laser radar, laser atmospheric transmission, free-space laser communication and other fields[1−4]. Therefore, coherent beam combining has become a research hotspot in the field of laser technology in recent years. The coherent combination technology based on Master Oscillator Power Amplifier (MOPA) structure adopts the modular structure, and realizes coherent beam combination through active phase control[5−6]. The commonly used active phase control methods mainly include heterodyne detection method[7], jitter method[8], simulated annealing algorithm[9] and Stochastic Parallel Gradient Descent (SPGD) algorithm[10−11]. The coherent combination system based on SPGD algorithm has low complexity and simple control strategy, and is expected to be a practical coherent combination scheme. The SPGD algorithm was first proposed by Voronstov *et al*. from the US Army Research Lab (ARL), and applied in the field of adaptive imaging[12]. In 2005, the ARL applied the SPGD algorithm to the fiber-laser optical phased array system to develop high-energy laser weapons[13]. In 2011, the University of Dayton in the United States cooperated with the ARL to control the beam phase by using the SPGD algorithm, and realized the coherent combination of seven 100-mW class fiber-laser targets in the loop with a transmission distance of 7 km[14]. In 2016, the research group realized the coherent combination of 21-beam fiber laser array with a transmission distance of 7 km by using the SPGD algorithm, and analyzed the system correction effect under different atmospheric turbulences[15]. In China, the National University of Defense Technology (NUDT), the Institute of Optics and Electronics, Chinese Academy of Sciences and other institutions have done in-depth research on SPGD-based coherent beam combination. In 2018,

GENG Chao *et al* from the Institute of Optics and Electronics, Chinese Academy of Sciences carried out the coherent combination experiment of a 7-cell fiber laser array with a transmission distance of 200 m. In this experiment, the target-in-loop method was combined with SPGD optimal control algorithm to suppress the turbulence effect very well and obtain a good combination effect[16]. In 2019, SU Rong-tao *et al*. from the NUDT realized the coherent combination of 60 fiber laser beams by using the SPGD algorithm. This is the highest number of fiber laser beams in coherent combination that has been reported in China, and is also the highest number of phase-controlled beams in a fiber laser array that has been reported internationally and calculated with an optimization algorithm[17]. In the same year, ZHI Dong *et al*. in that research group realized the efficient coherent combination of 6 fiber laser targets in the loop with a transmission distance of 0.8 km by using the SPGD algorithm (tilted phase control) and multi-jitter method (phase-locked control)[18]. At present, the analyses of the coherent combination system based on SPGD algorithm are mostly limited to the correction of static aberration or the study of remote coherent combination effect through off-site experiments. Few literatures have studied the correction effect of coherent combination system at different atmospheric Greenwood frequencies. In this paper, a set of rotating phase screens are used to simulate turbulent atmosphere and the correction effect of SPGD-based coherent combination system at different atmospheric Greenwood frequencies is studied by numerical simulation and experiment.

2 Fundamentals

In the gradient descent algorithm, if the objective function $J(\boldsymbol{u})$ drops at a fast speed, the change of the independent variable $\boldsymbol{u}$ should occur in the direction of current negative gradient:

$$\boldsymbol{u}^{(n+1)} = \boldsymbol{u}^{(n)} - \lambda \nabla J(\boldsymbol{u}^{(n)}), \tag{1}$$

where n is the number of iterations; and λ is the iteration step. λ is positive when the objective function $J(\boldsymbol{u})$ is at the minimum and negative when the objective function $J(\boldsymbol{u})$ is at the maximum. For each component:

$$u_j^{(n+1)} = u_j^{(n)} - \lambda \frac{\partial J(\boldsymbol{u}^{(n)})}{\partial u_j^{(n)}}. \tag{2}$$

SPGD algorithm is a special gradient descent algorithm, which uses stochastic parallel perturbation to estimate the gradient[19]. The evaluation function $J = J(\boldsymbol{u})$ of the system, which is the function of the phase control voltage $\boldsymbol{u} = \{u_1, u_2, \ldots, u_N\}$ applied to the beams, is taken as the optimization object of this algorithm. A set of small-perturbation signals $\delta\boldsymbol{u} = \{\delta u_1, \delta u_2, \ldots \delta u_N\}$ with a zero mean and fixed variance are actively applied to the phase control voltage. Then the variation of evaluation function δJ caused by stochastic disturbance voltage can be expressed as:

$$\delta J = J(\boldsymbol{u} + \delta\boldsymbol{u}) - J(\boldsymbol{u}). \tag{3}$$

The Taylor series expansion of equation (3) is:

$$\delta J = \sum_{j=1}^{N} \frac{\partial J}{\partial u_j} \delta u_j + \frac{1}{2} \sum_{j,k=1}^{N} \frac{\partial J}{\partial u_j \partial u_k} \delta u_j \delta u_k + \ldots . \tag{4}$$

By multiplying both sides of equation (4) by δu_j and calculating the mathematical expectation, we obtain:

$$\langle \delta J \delta u_i \rangle = \sum_{j}^{N} \frac{\partial J}{\partial u_j} \langle \delta u_j \delta u_i \rangle + \frac{1}{2} \sum_{j,k}^{N} \frac{\partial J}{\partial u_j \partial u_k} \langle \delta u_j \delta u_k \delta u_i \rangle + \ldots . \tag{5}$$

Stochastic parallel perturbation $\delta\boldsymbol{u} = \{\delta u_1, \delta u_2, \ldots \delta u_N\}$ is a statistically independent random variable with zero mean and equal variance. So

$$\langle \delta u_i \rangle = 0, \langle \delta u_i \delta u_j \rangle = \sigma^2 \delta_{ij}, \tag{6}$$

Moreover, the probability density distribution of $\{\delta u_j\}$ is symmetric with respect to the mean

value, that is,

$$\langle \delta u_i \delta u_j \delta u_k \rangle = 0. \quad (7)$$

Therefore, the equation (5) can be written as:

$$\langle \delta J \delta u_i \rangle = \frac{\partial J}{\partial u_i}\sigma^2 + o(\sigma^4). \quad (8)$$

Statistically averaged, $\delta J/\delta u_i$ can be used as an estimate of the gradient component $\partial J/\partial u_i$. By substituting equation (8) into equation (2), the iterative formula of SPGD algorithm can be obtained:

$$u_j^{(n+1)} = u_j^{(n)} - \gamma \delta J^{(n)} \delta u_j^{(n)}, \quad (9)$$

where $\gamma = \lambda/\sigma^2$ is the gain coefficient of SPGD algorithm.

The system structure using the SPGD algorithm to realize the coherent combination of two fiber laser beams is shown in Fig.1. First, the beam from the seed source is divided into two beams by a beam splitter, each of which passes through a phase modulator (for beam phase adjustment) and then a fiber amplifier (for beam power amplification). After the collimator collimation and lens focus, each beam is divided into two parts by beam splitter after passing through turbulent atmosphere (simulated by rotating phase screen). One part of the beam is received by CCD and then is used to observe the far-field pattern. The other part of the beam is detected by a single-point detector after attenuation (the attenuator is not shown in the Fig.1). Initially, when the phase controller is not run, the coherent combination system is in an open-loop state. Due to the influence of external environment and optical fiber amplifier, the phase of each beam fluctuates randomly. This will cause the random movement of interference pattern in the far field as well as the random change of the evaluation index detected by the single-point detector. When the SPGD algorithm is executed, the system is in a closed-loop state. According to the evaluation index detected by the single-point detector, the phase controller generates a set of control voltage signals to be applied to the phase modulator. After several iterations, the evaluation function no longer fluctuates randomly and drastically, and the interference pattern in the far field becomes stable. In this way, the system can reach the phase-locked state and achieve a relatively stable coherent combination output. In the coherent combination, the execution process of SPGD algorithm can be expressed as follows:

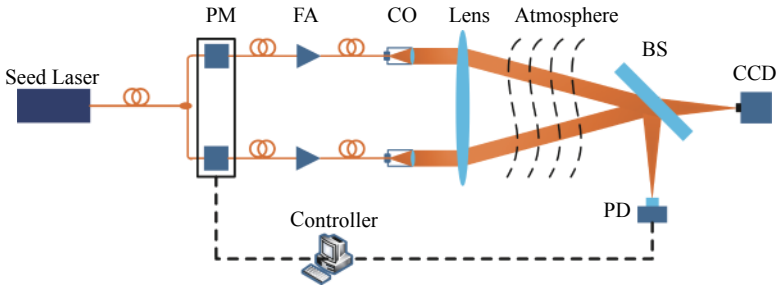

Fig. 1　The experimental scheme of coherent beam combining system of two fiber laser beams. PM: Phase Modulator; FA: Fiber Amplifiers; CO: Collimator; BS: Beam Splitting Mirror; PD: Photodetector

图 1　两路光纤激光相干合成系统结构图。PM: 相位调制器; FA: 光纤放大器; CO: 光纤准直器; BS: 分光镜; PD: 单点探测器。

(1) Set the gain coefficient and the initial phase control voltage $\boldsymbol{u}^{(0)} = \{u_1, u_2, \ldots, u_N\}$;

(2) Generate a set of stochastic disturbed voltages $\delta\boldsymbol{u}^{(k)} = \{\delta u_1, \delta u_2, \ldots \delta u_N\}$ that follow the Bernoulli distribution;

(3) Apply the disturbed voltage to the phase control voltage and obtain the evaluation functions $J_+(\boldsymbol{u}^{(k)} + \delta\boldsymbol{u}^{(k)})$ and $J_-(\boldsymbol{u}^{(k)} - \delta\boldsymbol{u}^{(k)})$;

(4) Calculate the variation of evaluation function δJ;

(5) Update the phase control voltage by using the equation (9);

(6) Repeat the steps (2) to (5) until the algorithm is ended.

3 Numerical simulation

In order to analyze the correction effect of the system on turbulent atmosphere at different atmospheric Greenwood frequencies, the coherent combination processes in free space and in turbulent atmosphere are simulated numerically in this section. The system parameters required for simulation are shown in Table 1. The spot radius of the unit beam is 2.5 mm, the distance between beam centers is 10 mm, the laser wavelength is 1 064 nm, and the transmission distance is 2 m. The Power-In-Bucket (PIB) of the far-field spot is taken as the evaluation function J of the combination system. Considering that in practical work, the thermal effect of gain medium (optical fiber) and the influence of external environment will cause the phase inconsistency of unit beams, the initial phase of each beam in the numerical simulation is assumed to follow the Gaussian distribution with the mean value of zero and the variance of 3π.

Tab. 1 System parameters used for simulation

表 1 仿真系统参数

Parameter	Value
Distance: L/m	2
Wavelength: λ/m	$1\,064 \times 10^{-9}$
Beam radius: w_0/m	2.5×10^{-3}
Number of samples:	256

In order to facilitate comparative analysis, this section normalizes the value of the system evaluation index PIB, and stipulates that the PIB value is 1 when the output of coherent combination system is stable under the free-space condition. Firstly, the influence of different turbulence intensities on coherent combination system was analyzed under static atmospheric conditions (the algorithm runs much faster than the atmospheric Greenwood frequency). The change of the system evaluation index PIB with turbulence intensity is shown in Fig.2. The numerical results show that with the increase of atmospheric turbulence intensity, the turbulence will aggravate the wavefront distortion, beam expansion, spot drift and other beam effects, so that the energy concentration of far-field spot will decrease and the combination effect of the coherent combination system will become worse.

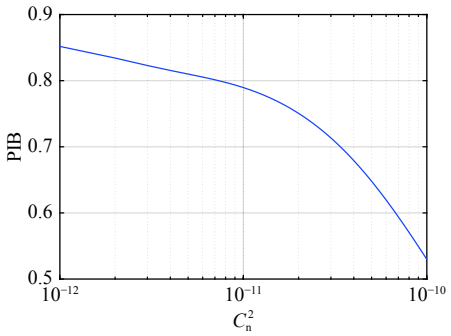

Fig. 2 System evaluation index PIB varies with iteration turbulence intensity

图 2 系统评价指标 PIB 随湍流强度的变化曲线

In this paper, the rotating phase screen generated by calculation is used to simulate the dynamic atmospheric turbulence[20]. The generation of rotating phase screen is shown in Fig.3. Firstly, the method of power spectrum inversion plus subharmonic low-frequency compensation is used to simulate the generation of a set of large phase screens obeying the Kolmogorov statistical law. Secondly, the center distance R between sub-phase screen and large phase screen, the size d of the sub-phase screen as well as the rotation angle θ within the time τ are determined. Then, the center of the sub-phase screen at the time t is determined according to the center distance R, and a $d \times d$ rectangle phase screen is selected at the center of the sub-phase screen. At $t+\tau$, the new sub-phase screen is determined according to the rotation angle. The relationship between

the Greenwood frequency f_G of turbulent atmosphere and the rotational speed of phase screen can be expressed as:

$$f_G = (0.102k^2v^{5/3}C_n^2)^{3/5}, \quad (10)$$

where $k = 2\pi/\lambda$ is wave number; $v = 2\pi n_{sp}R$, where n_{sp} is the rotational speed of phase screen.

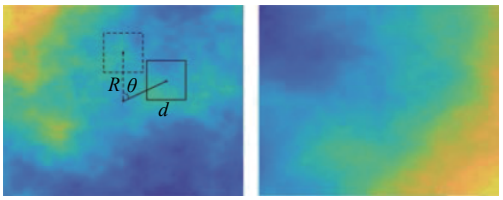

(a) 主相位屏
(a) Main phase screen

(b) $d\times d$ 子相位屏
(b) Sub-phase screen $d\times d$

Fig. 3　Schematic diagram of a rotating phase screen generation

图 3　旋转相位屏生成示意图

In order to facilitate the comparison with the experimental results, it is assumed that the running frequency of a single iteration of the algorithm is 350 Hz, the center distance R=30 mm, and the atmospheric refractive index structure constant $C_n^2 = 5\times10^{-11}\mathrm{m}^{-2/3}$. Under the condition of turbulent atmosphere, the change of the system evaluation index PIB with the number of iterations is shown in Fig.4. When the system is an open loop, the PIB value fluctuates randomly between 0.2 and 0.6 under the influence of turbulent atmosphere. When the system is a closed loop, the SPGD algorithm fails to make the combination system provide stable phase-locked output due to the continuous disturbance of turbulent atmosphere. However, the combination effect of the system using SPGD to control the beam phase is significantly better than that in the open-loop state. With the increase of atmospheric Greenwood frequency, the jitter amplitude and frequency of PIB value will increase, and the combination effect of the system will become worse. This shows that the coherent combination system based on SPGD algorithm has a significant correction effect on turbulent atmosphere, but the atmospheric Greenwood frequency has a great influence on the combination effect of the system.

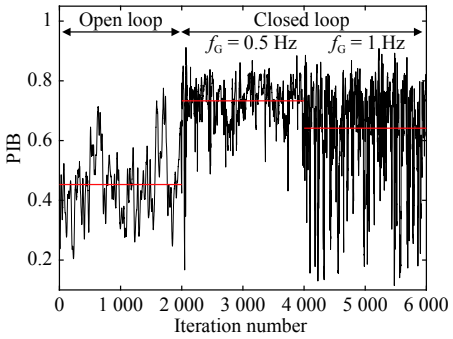

Fig. 4　System evaluation index PIB varies with iteration number under turbulent atmosphere

图 4　湍流大气下, 系统 PIB 随迭代次数的变化曲线

To quantitatively analyze the influence of atmospheric Greenwood frequency on the combination effect of the system, the change of the evaluation index PIB of coherent combination system with atmospheric Greenwood frequency has been obtained through simulation calculation, as shown in Fig. 5. The simulation results show that when the iteration frequency of the algorithm is much higher than atmospheric Greenwood frequency ($f_G < 0.5$ Hz), the convergence process of the algorithm will be less affected by turbulent atmosphere, and the amplitude of combination effect variation will be small. However, with the continuous increase of atmospheric Greenwood frequency, the turbulence of the outgoing beam by turbulent atmosphere will be quickened, and the PIB of the far-field spot will fluctuate more frequently. As a result, the SPGD algorithm can't timely and effectively adjust the control voltage of the phase modulator, resulting in worse and worse combination effect of the system. When the atmospheric Greenwood frequency is greater than 2 Hz, the change of the system evaluation index PIB tends to be gentle with the increase of atmospheric Greenwood frequency. This is because the disturbance by turbulent atmosphere is aggravated, the sensitivity of the control algorithm to external disturbance is reduced, and thus the closed-

loop control effect of the system is not obvious. The comparison between open-loop and closed-loop system states shows that the evaluation index of the system in the closed-loop state is higher than that in the open-loop state.

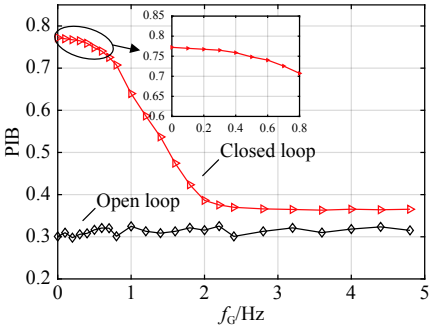

Fig. 5 Evaluation function varying with atmospheric Greenwood frequency

图 5 评价函数随大气格林伍德频率的变化曲线

4 Experiment and results

An experimental platform was built based on the structural diagram of coherent combination system shown in Fig. 1, and the SPGD algorithm was used to experimentally study the correction effect of coherent combination system on turbulent atmosphere. The central wavelength of the seed source is 1 064 nm, the line width is less than 20 kHz, and the maximum output power is 100 mW. The fiber amplifier is polarization-maintaining fiber amplifier with the maximum amplification factor of 10 times. The phase modulator is a lithium-niobate phase modulator made by French iXblue, with a half-wave voltage of 2 V. The detector is an InGaAs avalanche photodetector with an effective diameter of 0.2 mm. The SPGD algorithm controller is composed of NI acquisition card and LabView upper computer software. The time for each iteration operation in the algorithm is about 2.8 ms. In the experiment, Lexitek's static phase screen (its thickness is 22 mm, and the corresponding atmospheric coherence length is r_0 = 4.8 mm) was selected. It is a pseudo-random phase plate with Kolmogorov statistical law made by using the near-refractive-index matching of optical polymer and acrylic plastic and the related algorithm. The turbulent atmosphere is simulated as the rotational speed of the phase screen is controlled by a control box. The atmospheric refractive index structure constant can be obtained by equation (11) to be $C_n^2 = 8.8\times10^{-11}\mathrm{m}^{-2/3}$.

$$C_n^2 = 0.42 r_0^{-5/3} k^{-2}. \tag{11}$$

In order to analyze the influence of turbulent atmosphere on coherent combination, the coherent combination experiment without phase screen is first carried out in this paper. The change of the detector's output voltage with the running times (time) of the algorithm in the open-loop or closed-loop system is shown in Fig. 6. When the SPGD algorithm is not run, the system will be in an open-loop state and the evaluation index output by the detector will constantly change between 0.5 V and 0.7 V. When the SPGD algorithm is executed, the system will be in a closed-loop state. After several iterations, the voltage value output by the detector will basically stay around 0.8 V. It should be noted that in the closed-loop process of the system, the value of the system evaluation index PIB will fluctuate greatly for two reasons. First, the phase control voltage is out of the hardware voltage range, so the control voltage is reset, resulting in the loss of system locking. Second, the seed source or amplifier is unstable.

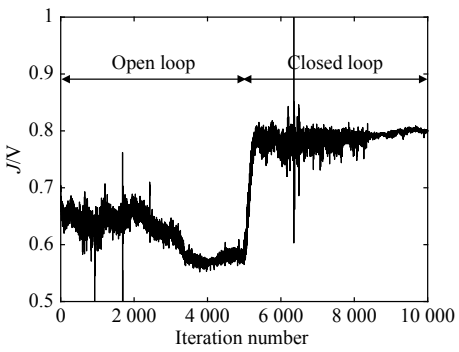

Fig. 6 Detector's output voltage varies with iteration number

图 6 探测器输出电压随算法迭代次数的变化曲线

When the phase screen is added, the relationship between the output voltage of the detector and the running times (time) of the algorithm at different Greenwood frequencies can be shown in Fig. 7. It can be found that the SPGD algorithm can achieve stable phase-locked output when the phase screen is stationary, i.e. the atmospheric Greenwood frequency is zero. Due to the effect of phase screen on the beam expansion and beam distortion, the combination effect of the system under atmospheric conditions is lower than that in free space. When the atmospheric Greenwood frequency is 0.32 Hz, the atmospheric disturbance can cause the unable convergence of SPGD algorithm and thus the unable phase-locked output of the system. However, by comparing the output voltages of the detector in the open-loop and closed-loop states, it can be seen that the average output voltage with the SPGD algorithm running is significantly higher than that in the open loop. The experimental results show that the coherent combination system using SPGD algorithm has a certain correction effect on turbulent atmosphere. However, the atmospheric Greenwood frequency has a greater influence on the combination effect of the system.

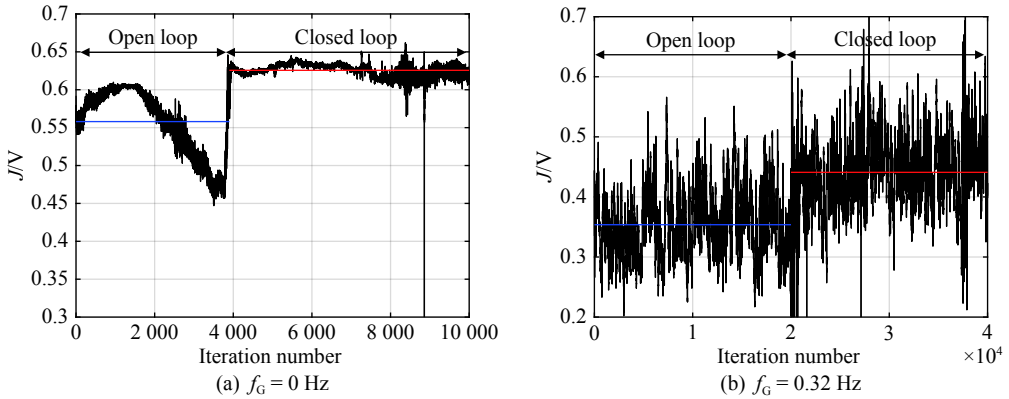

Fig. 7　Detector's output voltage varies with the number of iterations under different Greenwood frequencies

图 7　在不同的格林伍德频率下, 探测器的输出电压与迭代次数的变化曲线

The change of the detector 's output voltage with the Greenwood frequency of turbulent atmosphere when the system is in open and closed loops is shown in Fig. 8. It can be seen from the figure that when the Greenwood frequency is small, the continuous turbulence of the turbulent atmosphere causes the damage to the convergence of SPGD algorithm so that it cannot timely and effectively adjust the control voltage of the phase modulator. As a result, the voltage output by the detector decreases with the increase of Greenwood frequency. When the Greenwood frequency is greater than a certain value (0.5 Hz), the sensitivity of SPGD algorithm to external disturbance will decrease with the acceleration of atmospheric disturbance, and the output voltage of the detector will decrease slowly with the increase of Greenwood frequency. The changing trend of system combination effect relative to atmospheric Greenwood frequency basically matches the results of numerical simulation. In the low frequency (f_G < 0.5Hz) part, there are two reasons for the difference in the changing trend of the synthetic effect of experiment and simulation. On the one hand, due to the influence of dynamic noise in the system and external environment, the number of iterations required for the convergence of SPGD algorithm in the hardware (about 100 iterations) is greater than that required in the numerical simula-

tion (about 20 iterations). On the other hand, due to the limitation of experimental hardware, the iteration frequency of the algorithm is only 350 Hz, and the speed range of the control box is limited. Moreover, in this paper, there are insufficient samples for the experiment at lower atmospheric Greenwood frequency.

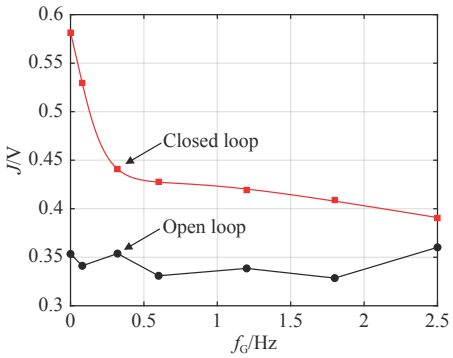

Fig. 8 Detector′s output voltage varies with Greenwood frequency when the system is open and closed

图 8 系统开环和闭环时探测器输出电压随大气湍流格林伍德频率的变化曲线

5 Conclusion

The random dynamic disturbance of turbulent atmosphere will cause the wavefront distortion and random phase change of light beam, which greatly limits the application of coherent combination system of fiber laser array in practice. Firstly, the influence of different atmospheric turbulence intensities on coherent combination system in static atmospheric environment (the algorithm runs much faster than the atmospheric Greenwood frequency) was analyzed in this paper. Then a set of rotating phase screens generated by numerical calculation were used to simulate turbulent atmosphere and to study the correction effect of the coherent combination system based on SPGD algorithm in turbulent atmosphere. The numerical results show that with the increase of atmospheric turbulence intensity, the far-field spot energy concentricity of the system will decline gradually. With the increase of atmospheric Greenwood frequency, the turbulent atmosphere will disturb the beam faster, and the convergence effect of the system will become worse and gradually level off. Finally, an experimental platform was built to simulate turbulent atmosphere by controlling the rotational speed of static phase screens, and to carry out the coherent combination of two laser beams. It can be concluded from the experimental results that under a certain iteration frequency (350 Hz) of the algorithm, with the acceleration of phase screen speed, the sensitivity of SPGD algorithm to atmospheric disturbance will continuously decline so that the average output voltage of the detector in the closed-loop system will decrease and tend to level off. The research on the correction effect of coherent combination system at different atmospheric Greenwood frequencies in this paper provides a reference for the application of the system in practice. In the future, we will further increase the iteration frequency of SPGD algorithm and the number of combined beams to study the impact of turbulent atmosphere on the system.

——中文对照版——

1 引 言

光纤激光相干合成即各子路光束的相干叠加，能在大幅度提高输出光功率的同时保证良好的光束质量，在激光雷达、激光大气传输、自由空间激光通信等领域具有广阔的应用前景[1-4]。因此，光纤激光相干合成技术近年来已成为激光技术领域的研究热点。基于主振荡功率放大器（MOPA）结构的相干合成技术采用模块化结构，

通过主动相位控制，实现各路光束的相干合成[5–6]。通常采用的主动相位控制方法主要有外差探测法[7]、抖动法[8]、模拟退火算法[9]以及随机并行梯度下降（SPGD）算法[10-11]等。基于 SPGD 算法的相干合成系统的系统复杂性较小，控制策略较简单，有望成为实用的相干合成方案。SPGD 算法最早是由美国陆军实验室的 Voronstov 等人提出的，并被应用在自适应成像领域[12]。2005 年，美国陆军实验室将 SPGD 算法应用到光纤激光光学相控阵系统中，发展高能激光武器[13]。2011 年美国戴顿大学与陆军实验室展开合作，利用 SPGD 算法控制光束相位，实现了传输距离为 7 km 的 7 路 100 mW 级的光纤激光目标在回路的相干合成[14]。2016 年，该课题组利用 SPGD 算法在 7 km 的传输距离下实现了 21 路光纤激光阵列的相干合成，并且对不同大气湍流下的系统校正效果进行了分析[15]。在国内，国防科技大学、中国科学院光电技术研究所等单位在基于 SPGD算法的光纤激光相干合成方面做了深入详细的研究。2018 年，中国科学院光电技术研究所的耿超等人开展了 7 单元光纤激光阵列 200 m 传输距离的相干合成实验，该实验采用目标在回路的方法结合 SPGD 优化控制算法，能够很好地抑制湍流效应，并取得了较好的合成效果[16]。2019 年，国防科技大学的粟荣涛等人利用 SPGD 算法实现了 60 路光纤激光的相干合成。这是国内公开报道的光纤激光相干合成的最高路数，也是国际上公开报道的光纤激光阵列最高的优化算法相位控制路数[17]。同年，该课题组的支东等人利用 SPGD 算法（倾斜相位控制）和多抖动法（锁相控制），实现了 0.8 公里传输距离的 6 路光纤激光目标在回路的高效相干合成[18]。通过大量调研发现，目前对基于 SPGD 算法的相干合成系统的分析大多限于对静态像差的校正或通过场外实验研究远距离的相干合成效果。鲜有文献对不同的大气格林伍德频率下相干合成系统的校正效果进行研究。本文利用旋转的相位屏模拟湍流大气，通过数值仿真和实验对在不同大气格林伍德频率下基于 SPGD 算法的相干合成系统的校正效果进行研究。

2　基本原理

在梯度下降算法中，若要目标函数 $J(\boldsymbol{u})$ 以较快的速度下降，自变量 $\boldsymbol{u}$ 的变化方向则要沿着此时的负梯度方向：

$$\boldsymbol{u}^{(n+1)} = \boldsymbol{u}^{(n)} - \lambda \nabla J(\boldsymbol{u}^{(n)}), \tag{1}$$

其中，n 为迭代次数；λ 为迭代步长，当目标函数 $J(\boldsymbol{u})$ 取极小值时，λ 为正值，当目标函数 $J(\boldsymbol{u})$ 取极大值时，λ 为负值。对于每一个分量有：

$$u_j^{(n+1)} = u_j^{(n)} - \lambda \frac{\partial J(\boldsymbol{u}^{(n)})}{\partial u_j^{(n)}}. \tag{2}$$

SPGD 算法是一种特殊的梯度下降算法，它采用随机并行扰动的方式进行梯度估计[19]。将系统的评价函数 J=$J(\boldsymbol{u})$ 作为算法的优化对象，它是施加在各路光束相位控制电压$\boldsymbol{u} = \{u_1, u_2, \ldots, u_N\}$上的函数。主动向相位控制电压施加一组均值为零方差固定的微小扰动信号$\delta\boldsymbol{u} = \{\delta u_1, \delta u_2, \ldots \delta u_N\}$。则随机扰动电压带来的评价函数变化量 δJ 可以表示为：

$$\delta J = J(\boldsymbol{u} + \delta\boldsymbol{u}) - J(\boldsymbol{u}). \tag{3}$$

将公式 (3) 进行泰勒级数展开：

$$\delta J = \sum_{j=1}^{N} \frac{\partial J}{\partial u_j} \delta u_j + \frac{1}{2} \sum_{j,k=1}^{N} \frac{\partial J}{\partial u_j \partial u_k} \delta u_j \delta u_k + \ldots \tag{4}$$

在公式 (4) 两边同时乘以 δu_j，并求数学期望，可以得到：

$$\begin{aligned} \langle \delta J \delta u_i \rangle = & \sum_{j}^{N} \frac{\partial J}{\partial u_j} \langle \delta u_j \delta u_i \rangle + \\ & \frac{1}{2} \sum_{j,k}^{N} \frac{\partial J}{\partial u_j \partial u_k} \langle \delta u_j \delta u_k \delta u_i \rangle + \ldots \end{aligned} \tag{5}$$

对于随机并行扰动$\delta\boldsymbol{u} = \{\delta u_1, \delta u_2, \ldots \delta u_N\}$，它是均值为零、方差相等、统计独立的随机变量。所以有：

$$\langle \delta u_i \rangle = 0, \langle \delta u_i \delta u_j \rangle = \sigma^2 \delta_{ij}, \tag{6}$$

而且，$\{\delta u_j\}$的概率密度分布是关于均值对称的，有：

$$\langle \delta u_i \delta u_j \delta u_k \rangle = 0, \tag{7}$$

所以公式 (5) 可以写为:

$$\langle \delta J \delta u_i \rangle = \frac{\partial J}{\partial u_i}\sigma^2 + o(\sigma^4). \tag{8}$$

从统计意义上平均, 可将 $\delta J/\delta u_i$ 作为梯度分量 $\partial J/\partial u_i$ 的估计值。将公式 (8) 代入公式 (2) 中, 可以得到 SPGD 算法的迭代公式:

$$u_j^{(n+1)} = u_j^{(n)} - \gamma \delta J^{(n)} \delta u_j^{(n)}, \tag{9}$$

其中, $\gamma=\lambda/\sigma^2$ 为 SPGD 算法的增益系数。

利用 SPGD 算法实现 2 路光纤激光相干合成的系统结构图如图 1 所示。由种子源发出的光束被分束器分成两路, 每一路光束先后经过相位调制器(调节光束相位)和光纤放大器(放大光束功率)。各路光束经过准直器准直和透镜聚焦后, 再经过湍流大气(由旋转的相位屏模拟), 之后被分光镜分成两部分。一部分光被 CCD 接收, 用于观察远场图样; 另一部分光经过衰减(衰减片图中未显示)后, 被单点探测器所探测。最初, 没有使用相位控制器时, 相干合成系统处于开环状态。受外部环境和光纤放大器的影响, 每路光束的相位随机波动。这就会造成远场干涉图样的随机移动, 同时单点探测器探测的评价指标也会随机变化。当使用 SPGD 算法时, 系统处于闭环状态。相位控制器根据单点探测器探测的评价指标, 生成一组控制电压信号, 施加到相位调制器上。经过多次迭代后, 评价函数不再大幅度随机波动, 远场的干涉图样也逐渐稳定。系统最终达到锁相状态, 可以实现较为稳定的相干合成输出。在相干合成中, SPGD 算法的执行过程可以表示为:

(1) 设置增益系数和初始相位控制电压 $\boldsymbol{u}^{(0)} = \{u_1, u_2, \ldots, u_N\}$;

(2) 生成一组服从伯努利分布的随机扰动电压 $\delta\boldsymbol{u}^{(k)} = \{\delta u_1, \delta u_2, \ldots \delta u_N\}$;

(3) 将扰动电压施加到相位控制电压上, 并得到评价函数 $J_+(\boldsymbol{u}^{(k)}+\delta\boldsymbol{u}^{(k)})$ 以及 $J_-(\boldsymbol{u}^{(k)}-\delta\boldsymbol{u}^{(k)})$;

(4) 计算评价函数的变化量 δJ;

(5) 利用公式 (9) 更新相位控制电压;

(6) 重复步骤 (2) 到 (5), 直至算法结束。

3 数值模拟

为了分析不同大气格林伍德频率下系统对湍流大气的校正效果, 本节分别对自由空间和湍流大气下的相干合成过程进行数值模拟。仿真所需的系统参数如表 1 所示。取单元光束的光斑半径为 2.5 mm, 光束中心间距为 10 mm, 激光波长为 1 064 nm, 传输距离为 2 m, 取远场光斑的桶中功率 (PIB) 作为合成系统的评价函数 J。考虑到在实际工作中, 受光纤增益介质热效应以及外界环境因素的影响, 各激光单元光束相位不一致, 在进行数值仿真时, 假设各路初始相位服从均值为零方差为 3π 的高斯分布。

为了便于对比分析, 本节对系统评价指标 (PIB 值) 进行了归一化处理, 规定在自由空间条件下相干合成系统稳定输出时的 PIB 值为 1。首先, 在静态大气环境(算法的运行速率远远大于大气格林伍德频率)下分析不同大气湍流强度对相干合成系统的影响。系统评价指标 PIB 随湍流强度的变化曲线如图 2 所示。数值计算结果表明, 随着大气湍流强度的增加, 湍流使光束产生的波前畸变、光束扩展以及光斑漂移等效应加剧, 导致远场光斑能量集中度下降, 相干合成系统的合成效果变得越来越差。

本文利用计算生成的旋转相位屏来模拟动态大气湍流[20]。旋转相位屏生成示意图如图 3 所示。首先, 利用功率谱反演加次谐波低频补偿方法模拟产生一组符合 Kolmogorov 统计规律的大相位屏。其次, 确定子相位屏与大相位屏的中心距离 R、子相位屏的尺寸 d 以及时间 τ 内的旋转角度 θ。然后, 根据中心距离 R 确定 t 时刻, 子相位屏的中心, 在子相位屏的中心位置处选取大小为 $d\times d$ 的矩形相位屏。在 $t+\tau$ 时刻, 根据旋转角度确定新的子相位屏。湍流大气格林伍德频率 f_G 与相位屏转速的关系可以表示为:

$$f_G = (0.102k^2 v^{5/3} C_n^2)^{3/5}, \tag{10}$$

其中, $k=2\pi/\lambda$ 为波数; $v=2\pi n_{sp}R$, 式中 n_{sp} 为相位屏的转速。

为了便于与实验结果做对比分析，假设算法单次迭代的运行频率为 350 Hz，中心间距 R=30 mm，大气折射率结构常数 C_n^2=5×10^{-11}m$^{-2/3}$。在湍流大气下，系统评价指标 PIB 随迭代次数的变化曲线如图 4 所示。当系统开环时，受湍流大气的影响，PIB 值在 0.2 到 0.6 之间随机波动；当系统闭环时，由于湍流大气的持续扰动，SPGD 算法未能使合成系统实现稳定的锁相输出。不过，利用 SPGD 控制光束相位后，系统的合成效果明显好于开环状态下的合成效果。增加大气格林伍德频率，系统的 PIB 值抖动幅度和频率变大，系统的合成效果变差。这表明，基于 SPGD 算法的相干合成系统对湍流大气具有明显的校正效果，但是大气格林伍德频率的大小对系统合成效果的影响较大。

为了便于定量分析湍流大气的格林伍德频率对系统合成效果的影响，通过仿真计算得出了相干合成系统的评价指标 PIB 随大气格林伍德频率的变化曲线，如图 5 所示。仿真结果表明：当算法的迭代频率远大于大气格林伍德频率(f_G<0.5 Hz)时，算法的收敛过程受湍流大气的影响较小，系统的合成效果变化幅度较小；但是随着大气格林伍德频率的继续增加，湍流大气对出射光束的扰动加快，远场光斑的 PIB 波动频率增加，使 SPGD 算法不能及时有效地调整相位调制器的控制电压，导致系统的合成效果越来越差；当大气格林伍德频率大于 2 Hz 时，随着大气格林伍德频率的增加，系统的评价指标 PIB 变化趋于平缓。这是因为湍流大气的扰动加剧，控制算法对外界扰动的敏感度降低，使得系统的闭环控制效果不明显。闭环状态下系统的评价指标高于开环下的评价指标。

4　实验与结果

基于图 1 的光纤激光相干合成系统结构图搭建实验平台，利用 SPGD 算法开展相干合成系统对湍流大气校正效果的实验研究。种子源的中心波长为 1 064 nm，线宽小于 20 kHz，最大输出功率为 100 mW。光纤放大器为保偏光纤放大器，最大放大倍数为 10 倍。相位调制器为法国 iXblue 公司的铌酸锂相位调制器，半波电压为 2 V。探测器为铟镓砷雪崩光电探测器，探测有效直径为 0.2 mm。SPGD 算法控制器由 NI 采集卡和 LabView 上位机软件组成，算法一次迭代时间约为 2.8 ms。实验采用 Lexitek 公司的静态相位屏（厚度为 22 mm，对应的大气相干长度 r_0=4.8 mm），它是利用光学聚合物加丙烯酸塑料的近折射率匹配技术结合相关算法制成的符合 Kolmogorov 统计规律的伪随机大气相位板，通过控制箱控制相位屏的转速来模拟湍流大气。大气折射率结构常数可以由式 (11) 求得，为C_n^2 = 8.8×10^{-11}m$^{-2/3}$.

$$C_n^2 = 0.42 r_0^{-5/3} k^{-2}. \tag{11}$$

为了便于分析湍流大气对相干合成效果的影响，本文首先开展了不加相位屏时系统的相干合成实验。系统在开环和闭环状态下探测器输出的电压随算法运行次数(时间)的变化曲线如图 6 所示。当 SPGD 算法没有运行时，系统处于开环状态，探测器输出的评价指标在 0.5 ~ 0.7 V 之间不断变化。当 SPGD 算法运行时，系统处于闭环状态，经过多次迭代，探测器输出的电压值基本稳定在 0.8 V 附近。需要说明的是，在系统闭环过程中，系统的评价指标 (PIB 值) 出现了大幅度波动。一方面是因为相位控制电压超出了硬件电压范围，控制电压被重置，导致系统失锁；另一方面是种子源或放大器的不稳定。

加入相位屏时，系统在不同的格林伍德频率下，探测器输出的电压与算法运行次数(时间)的关系如图 7 所示。可以发现，当相位屏静止，即大气格林伍德频率为零时，SPGD 算法可以实现稳定的锁相输出。由于相位屏对传输光束有光束扩展效应以及受光束畸变效应的影响，系统在大气条件下的合成效果低于自由空间下的合成效果。当大气格林伍德频率为 0.32 Hz 时，大气扰动使 SPGD 算法不能稳定收敛，导致系统无法实现稳定锁相输出。但是对比开环和闭环状态下探测器的输出电压，可以看出，运行 SPGD 算法时的输出电压均值明显高于开环下的输出电压均值。实验结果表明，应用 SPGD 算法的相干合成系统对湍流大气有一定的校正效果。但是大气格林伍德频率对系统的合成效果影响较大。

系统在开环和闭环两种状态下探测器输出电压随湍流大气格林伍德频率的变化曲线如图 8 所示。从图中可以看出，在格林伍德频率较小时，由于湍流大气的持续扰动，SPGD 算法的收敛性遭到破坏，其不能及时有效地调整相位调制器的控制电压，导致探测器输出的电压值随着格林伍德频率的增加而减小；在格林伍德频率大于一定值（0.5 Hz）时，随着大气扰动的加快，SPGD 算法对外界扰动的敏感度降低，探测器的输出电压随着格林伍德频率的增加而缓慢减小。系统的合成效果随着大气格林伍德频率的变化趋势与数值仿真结果基本相符。在低频（$f_G < 0.5$Hz）部分，实验与仿真合成效果的变化趋势存在差异。一方面是因为实验中系统和外界环境动态噪声的影响，SPGD 算法在硬件中收敛所需的迭代次数（100 次左右）大于在数值仿真中所需的迭代次数（20 次左右）；另一方面由于实验硬件的限制，算法的迭代频率只有 350 Hz，而且控制箱的转速范围有限，本文实验部分对于较低大气格林伍德频率的实验样本数不足。

5 结 论

湍流大气对光束的随机动态扰动会造成光束波前畸变和相位随机变化，这极大地限制了光纤激光相干合成系统的实际应用。本文首先分析了静态大气环境（算法的运行速率远远大于大气格林伍德频率）下不同大气湍流强度对相干合成系统的影响；然后，利用数值计算生成的旋转的相位屏来模拟湍流大气，研究基于 SPGD 算法的相干合成系统在湍流大气下的校正效果。数值结果表明，随着大气湍流强度的增加，系统的远场光斑能量集中度逐渐下降；随着大气格林伍德频率的增加，湍流大气对光束的扰动加快，系统的收敛效果变差并逐渐趋于平缓。最后，搭建实验平台，通过控制静态相位屏的转速来模拟湍流大气，进行了两路光纤激光相干合成实验。由实验结果可以得出，在算法迭代频率（350 Hz）一定的条件下，随着相位屏转速的加快，由于 SPGD 算法对大气扰动的敏感度不断降低，系统闭环时探测器输出的电压均值不断减小并趋于平缓。本文对不同大气格林伍德频率下光纤激光相干合成系统的校正效果展开研究，为系统在实际中的应用提供了参考。今后，我们将进一步提高 SPGD 算法的迭代频率以及增加光束合成数目，更深入地研究湍流大气对系统的影响。

参考文献：

[1] 王小林, 周朴, 粟荣涛, 等. 高功率光纤激光相干合成的现状、趋势与挑战[J]. 中国激光, 2017, 44(2): 3-28.
WANG X L, ZHOU P, SU R T, *et al*.. Current situation, tendency and challenge of coherent combining of high power fiber lasers[J]. *Chinese Journal of Lasers*, 2017, 44(2): 3-28. (in Chinese)

[2] LIU Z J, ZHOU P, XU X J, *et al*.. Coherent beam combining of high power fiber lasers: progress and prospect[J]. *Science China Technological Sciences*, 2013, 56(7): 1597-1606.

[3] 曾昊旻, 李松, 张智宇, 等. 车载激光雷达Risley棱镜光束扫描系统[J]. 光学精密工程, 2019, 27(7): 1444-1450.
ZENG H M, LI S, ZHANG ZH Y, *et al*.. Risley-prism-based beam scanning system for mobile lidar[J]. *Optics and Precision Engineering*, 2019, 27(7): 1444-1450. (in Chinese)

[4] 王惠琴, 宋梨花, 曹明华, 等. 湍流信道下光空间调制信号的压缩感知检测[J]. 光学精密工程, 2018, 26(11): 2669-2674.
WANG H Q, SONG L H, CAO M H, *et al*.. Compressed sensing detection of optical spatial modulation signal in turbulent channel[J]. *Optics and Precision Engineering*, 2018, 26(11): 2669-2674. (in Chinese)

[5] 程雪, 王建立, 刘昌华. 高能光纤激光器光束合成技术[J]. 红外与激光工程, 2018, 47(1): 0103011.
CHEN X, WANG J L, LIU CH H. Beam combining of high energy fibre lasers[J]. *Infrared and Laser Engineering*, 2018, 47(1): 0103011. (in Chinese)

[6] WANG X L, ZHOU P, MA Y X, *et al*.. Active phasing a nine-element 1.14 kW all-fiber two-tone MOPA array using

SPGD algorithm[J]. *Optics Letters*, 2011, 36(16): 3121-3123.

[7] GOODNO G D, KOMINE H, MCNAUGHT S J, *et al*.. Coherent combination of high-power, zigzag slab lasers[J]. *Optics Letters*, 2006, 31(9): 1247-1249.

[8] MA Y X, ZHOU P, WANG X L, *et al*.. Coherent beam combination with single frequency dithering technique[J]. *Optics Letters*, 2010, 35(9): 1308-1310.

[9] 周朴, 马阎星, 王小林, 等. 模拟退火算法光纤放大器相干合成[J]. 强激光与粒子束, 2010, 22(5): 973-977.
ZHOU P, MA Y X, WANG X L, *et al*.. Coherent beam combining of fiber amplifiers based on stimulated annealing algorithm[J]. *High Power Laser and Particle Beams*, 2010, 22(5): 973-977. (in Chinese)

[10] ZHOU P, LIU Z J, WANG X L, *et al*.. Coherent beam combining of two fiber amplifiers using stochastic parallel gradient descent algorithm[J]. *Optics & Laser Technology*, 2009, 41(7): 853-856.

[11] ZHOU P, MA Y X, WANG X L, *et al*.. Coherent beam combination of three two-tone fiber amplifiers using stochastic parallel gradient descent algorithm[J]. *Optics Letters*, 2009, 34(19): 2939-2941.

[12] VORONTSOV M A, CARHART G W, RICKLIN J C. Adaptive phase-distortion correction based on parallel gradient-descent optimization[J]. *Optics Letters*, 1997, 22(12): 907-909.

[13] VORONTSOV M. Adaptive Photonics Phase-Locked Elements (APPLE): system architecture and wavefront control concept[J]. *Proceedings of SPIE*, 2005, 5895: 589501.

[14] WEYRAUCH T, VORONTSOV M, CARHART G, *et al*.. Experimental demonstration of coherent beam combining over a 7 km propagation path[J]. *Optics Letters*, 2011, 36(22): 4455-4457.

[15] VORONTSOV M, FILIMONOV G, OVCHINNIKOV V, *et al*.. Comparative efficiency analysis of fiber-array and conventional beam director systems in volume turbulence[J]. *Applied Optics*, 2016, 55(15): 4170-4185.

[16] 耿超, 杨燕, 李枫, 等. 光纤激光相干合成研究进展[J]. 光电工程, 2018, 45(3): 170692.
GENG CH, YANG Y, LI F, *et al*.. Research progress of fiber laser coherent combining[J]. *Opto-Electronic Engineering*, 2018, 45(3): 170692. (in Chinese)

[17] 粟荣涛, 马阎星, 奚加超, 等. 60路大阵元光纤激光高效相干合成[J]. 红外与激光工程, 2019, 48(1): 331.
SU R T, MA Y X, XI J CH, *et al*.. 60-channel large array element fiber laser high efficiency coherent synthesis[J]. *Infrared and Laser Engineering*, 2019, 48(1): 331. (in Chinese)

[18] 支冬, 马阎星, 马鹏飞, 等. 公里级湍流大气环境下光纤激光高效相干合成[J]. 红外与激光工程, 2019, 48(10): 1005007.
ZHI D, MA Y X, MA P F, *et al*.. Efficient coherent beam combining of fiber laser array through km-scale turbulent atmosphere[J]. *Infrared and Laser Engineering*, 2019, 48(10): 1005007. (in Chinese)

[19] 刘磊, 郭劲, 赵帅, 等. 随机并行梯度下降算法在激光束整形中的应用[J]. 中国光学, 2014, 7(2): 260-266.
LIU L, GUO J, ZHAO SH, *et al*.. Application of stochastic parallel gradient descent algorithm in laser beam shaping[J]. *Chinese Optics*, 2014, 7(2): 260-266. (in Chinese)

[20] 李盾, 宁禹, 吴武明, 等. 旋转相位屏的动态大气湍流数值模拟和验证方法[J]. 红外与激光工程, 2017, 46(12): 1211003.
LI D, NING Y, WU W M, *et al*.. Numerical simulation and validation method of atmospheric turbulence of phase screen in rotation[J]. *Infrared and Laser Engineering*, 2017, 46(12): 1211003. (in Chinese)

Author Biographics：

SONG Ji-kun (1992 —), male, born in Heze County, Shandong Province. He is a doctoral candidate. In 2015, he obtained his bachelor's degree from Shandong Jianzhu University. He is mainly engaged in the research of beam transmission and control. E-mail: song_jk@126.com

宋纪坤 (1992—), 男, 山东菏泽人, 博士研究生, 2015 年于山东建筑大学获得学士学位, 主要从事光束传输与控制方面的研究。E-mail: song_jk@126.com

WANG Ting-feng (1977—), male, born in Wendeng City, Shandong Province. He is a doctor, researcher and doctoral supervisor. He obtained his bachelor's degree from former Jilin University of Technology in 1999, master's degree from Jilin University in 2002, and doctor's degree from Changchun Institute of Optics, Fine Mechanics and Physics, CAS in 2005. He is mainly engaged in the research of laser application and photoelectricity. E-mail: wangtingfeng@ciomp.ac.cn

王挺峰 (1977—), 男, 山东文登人, 博士, 研究员, 博士生导师, 1999 年于原吉林工业大学获得学士学位, 2002 年于吉林大学获得硕士学位, 2005 年于中国科学院长春光学精密机械与物理研究所获得博士学位, 主要从事激光应用与光电总体方面的研究。E-mail: wangtingfeng@ciomp.ac.cn